Isı Bilimi ve Tekniği Dergisi, 40, 2, 293-308, 2020
J. of Thermal Science and Technology
©2020 TIBTD Printed in Turkey
ISSN 1300-3615
https://doi.org/10.47480/isibted.817047

A CONCISE ANALYTICAL TREATMENT OF ELASTIC RESPONSE OF A COOLING TWO-LAYER SOLID CYLINDER WITH DIFFERENT END AND BOUNDARY CONDITIONS

Tolga AKIŞ* and Ahmet N. ERASLAN**
* Department of Civil Engineering, Atılım University
06830 İncek, Ankara, tolga.akis@atilim.edu.tr, ORCID: 0000-0002-6754-4497
** Department of Engineering Sciences, Middle East Technical University
06531 Ankara, aeraslan@metu.edu.tr, ORCID: 0000-0002-1158-0042

(Geliş Tarihi: 29.07.2019, Kabul Tarihi: 18.08.2020)

Abstract: Analytical models are developed to estimate the transient elastic response of cooling two-layer solid cylinders with different end and boundary conditions. Such cylinders contain two layers that are in perfect contact. The hot assembly loses energy from its surface to either zero ambient by convection or by a prescribed lower surface temperature. In any case, as the cooling takes place slowly, the problem is amenable to use of the uncoupled theory of elasticity. A generalized plane strain solution is derived and then reduced to the state of plane strain by simply setting the axial strain equal to zero. The results of these solutions revealed that the radial and circumferential stresses remain unchanged by end conditions when the boundaries are free. However, in case of plane strain, the axial stress becomes the dominant stress component and it is much larger than that in free ends. Radially constrained boundaries create very large stresses in the assembly but the corresponding stress state is far away from yielding.
Keywords: Two-layer solid cylinder, Transient heat conduction, Cooling, Thermoelasticity, Generalized plane strain.

İKİ KATMANLI DOLU BİR SİLİNDİRİN ELASTİK DAVRANIŞININ FARKLI UÇ VE SINIR KOŞULLARI İÇİN ANALİTİK OLARAK İNCELENMESİ

Özet: İki katmanlı dolu silindirlerin zamana bağlı termoelastik davranışlarının farklı uç ve sınır koşulları için belirlenmesi amacıyla analitik modeller geliştirilmiştir. Söz konusu silindirler, aralarında mükemmel temas olan iki katmandan oluşmaktadır. Başlangıçta sıcak olan silindir, yüzeyinden konveksiyon yolu ile sıfır derecelik çevresel sıcaklığa veya önceden daha düşük olarak belirlenen yüzey sıcaklığına ulaşana kadar enerji kaybetmektedir. Tüm durumlarda soğuma yavaş bir biçimde gerçekleştiğinden problemde kuplajsız elastisite teorisinin kullanılması mümkün olmuştur. Genelleştirilmiş düzlemsel şekil değiştirme çözümü elde edilmiş ve bu çözüm, eksenel yöndeki birim şekil değiştirmeyi sıfıra eşitleyerek düzlemsel şekil değiştirme durumuna ait çözüme indirgenmiştir. Bu çözümlere ait sonuçlar, sınır koşullarının serbest olduğu durumlarda radyal ve teğetsel yöndeki gerilmelerin uç koşullarına göre değişmediğini göstermiştir. Ancak düzlemsel şekil değiştirme durumunda, eksenel gerilme baskın gerilme olmakta ve uçların serbest olduğu duruma göre oldukça yüksek değerlere ulaşmaktadır. Kompozit silindirin eksenel ve radyal yönde yer değiştirmesinin kısıtlanması büyük gerilmelere yol açmasına rağmen ilgili gerilme durumu silindirde akmaya yol açmamaktadır.
Anahtar Kelimeler: İki katmanlı dolu silindir, Zamana bağlı ısı iletimi, Soğuma, Termoelastisite, Genelleştirilmiş düzlemsel şekil değiştirme.

NOMENCLATURE

a, b	interface and outer radii of the assembly, respectively [m]	h	convection heat transfer coefficient [$W/(m^2\ ^0K)$]
α	coefficient of thermal expansion [$\bar{\alpha}_j = E_1\alpha_j T_0/\sigma_{01}$]	k	thermal conductivity [$W/(m\ ^0K)$]
α_T	thermal diffusivity [m^2/s]	ν	Poisson's ratio
C_i	integration constants	r, θ, z	cylindrical coordinates
E	modulus of elasticity [GPa]	σ_0	uniaxial yield stress [MPa]
ε_i	strain components [$\bar{\varepsilon}_j = \varepsilon_j E_1/\sigma_{01}$]	σ_i	stress components [$\bar{\sigma}_j = \sigma_j/\sigma_{01}$]
		$\bar{\sigma}_{vM}$	von Mises stress
		t	time [$\tau = \alpha_{T1}t/b$]
		T	temperature [$\bar{T}_j = T_j/T_0$]

T_C	temperature of the casing [^0C]
T_0	initial temperature [^0C]
u	radial displacement [$\bar{u} = E_1 u/(\sigma_{01} b)$]

INTRODUCTION

Basic structural elements such as disks, cylinders, tubes, spherical shells and plates have been commonly used in different branches of industry and in daily life. The composite versions of these elements are also used especially in mechanical, aerospace, and automotive engineering. Due to this reason, a detailed knowledge of the stress response of such components under different loading and boundary conditions is needed for various engineering applications.

The existence of temperature gradients in the elements constitutes an important and unavoidable class of loads as it may occur for many reasons. Consequently, theoretical and experimental investigations of thermally induced stresses and deformations in the above mentioned assemblies have extensively been studied by researchers. Being one of the classical problems of thermal sciences, the transient heat conduction in homogenous solid and hollow circular cylinders, slabs and solid and hollow spheres have been investigated by many researchers in the past. Solutions of some of these classical problems with different methods can be found in books Carslaw and Jaeger (1959), Boley and Weiner (1960), Noda et al. (2003), Hetnarski and Eslami (2009), and Hahn and Özışık (2012).

The transient temperature response of composite solids has been handled using different methods. The common analytical techniques used are Green functions, orthogonal expansions and the Laplace transformation (Hahn and Özışık, 2012). Applications of these techniques and the use of other approaches can be found in the studies of Monte (2002), Sun and Wichman (2004), and Lu et al. (2006a). Other related investigations with different geometries and boundary conditions can be found in Lu et al. (2006b), Lu and Viljanen (2006), and Singh et al. (2008).

The thermomechanical response due to heat conduction in homogenous solid and hollow elements such as cylinders and spheres were studied by several researchers in the past. These are by Ishikawa (1978), by Tanigava et al. (1984), by Thomas et al. (1985), and by Kandil et al. (1995). A collection of solutions to the thermoelastic response of cylinders, plates and spheres in transient heat conduction can be found in Noda et al. (2003) .

Recently, Eraslan and Apatay (2015) investigated the thermoelastic stresses in cylindrical rods subjected to periodic boundary conditions by Duhamel's theorem. In the following investigation by the same authors (Eraslan and Apatay, 2016), they extended their analytical model to include partially plastic deformation and sudden unloading of the solid cylinder by the use of classical theories of plasticity. The application of a similar procedure to the solution of loading and unloading problem of periodic heat generating cylinder can be found in Eraslan and Apatay (2017). On the other hand, transient response of an infinitely long annular cylinder composed of two different materials was studied by Yu-Ching and Cha'o-Kuang (1986), Jane and Lee (1999), Lee et al. (2001), Wang et al. (2004), Lee (2006), and Mashat et al. (2010).

The transient thermoelastic two-layer solid cylinder problem has been treated in an earlier work by Pardo et al. (1987). Following the approaches of Özışık (1980) for the transient heat transfer part and Boley and Weiner (1960) for the thermoelastic part two different problems have been solved. A composite circular disk with insulated ends (plane stress problem) and an infinitely long cylinder with fixed ends (plane strain problem). In this work, we extend their study to include the state of generalized plane strain, radially constrained boundaries and the use of physical properties of real engineering materials. In the following sections we describe the problems handled, present our analytical models, their detailed solutions and numerical results as the assemblies cool down slowly with different modes of heat transfer.

THERMOELASTIC MODEL AND ITS SOLUTION

Temperature Distribution for Convective Boundary Condition

The coordinate system and the dimensions of the two-layer solid cylinder are depicted in Fig. 1. An infinitely long cylinder contains an inner region $0 \le r \le a$ and an outer region $a \le r \le b$ that are in perfect contact as shown in Fig. 1. Initially both cylinders are at temperature $T_0 > 0$. For times $t > 0$ the cylinder loses energy from its surface by convection to the zero ambient temperature. The temperature distribution in the inner and outer regions are governed by unsteady heat conduction equations as (Hahn and Özışık, 2012)

$$\frac{\partial T_1}{\partial t} = \frac{\alpha_{T1}}{r}\left[\frac{\partial T_1}{\partial r} + r\frac{\partial^2 T_1}{\partial r^2}\right] \quad \text{in} \quad 0 \le r < a\,,\ t > 0 \qquad (1)$$

$$\frac{\partial T_2}{\partial t} = \frac{\alpha_{T2}}{r}\left[\frac{\partial T_2}{\partial r} + r\frac{\partial^2 T_2}{\partial r^2}\right] \quad \text{in} \quad a < r < b\,,\ t > 0 \qquad (2)$$

where $T_1(r,t)$ and $T_2(r,t)$ are the temperature distributions in the inner ($0 \le r \le a$) and outer ($a \le r \le b$) regions, respectively, and α_{T1} is the thermal diffusivity of the inner while α_{T2} is that of the outer region.

The boundary conditions are

$T_1(0,t) =$ finite

$$k_2 \frac{\partial T_2(b,t)}{\partial r} + hT_2(b,t) = 0 \tag{3}$$

The interface conditions are

$$\begin{aligned} &T_1(a,t) = T_2(a,t) \\ &k_1 \frac{\partial T_1(a,t)}{\partial r} = k_2 \frac{\partial T_2(a,t)}{\partial r} \end{aligned} \tag{4}$$

Finally, the initial conditions are

$$\begin{aligned} &T_1(r,0) = T_0, \quad 0 \le r \le a \\ &T_2(r,0) = T_0, \quad a \le r \le b \end{aligned} \tag{5}$$

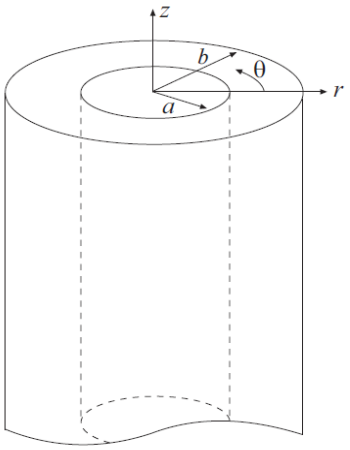

Figure 1. The cylindrical coordinate system and the dimensions of the long cylinder.

The solution is realized by separation of variables as

$$T_1(r,t) = \theta_1(t)R_1(r) \text{ and } T_2(r,t) = \theta_2(t)R_2(r) \tag{6}$$

Substituting into Eqs. (1) and (2) one obtains

$$\begin{aligned} &\frac{1}{\theta_{1n}} \frac{d\theta_{1n}}{dt} = \frac{\alpha_{T1}}{R_{1n} r} \left[\frac{dR_{1n}}{dr} + r \frac{d^2 R_{1n}}{dr^2} \right] = -\lambda_n^2 \\ &\frac{1}{\theta_{2n}} \frac{d\theta_{2n}}{dt} = \frac{\alpha_{T2}}{R_{2n} r} \left[\frac{dR_{2n}}{dr} + r \frac{d^2 R_{2n}}{dr^2} \right] = -\lambda_n^2 \end{aligned} \tag{7}$$

in which λ_n, $n = 1,2,...$ are the eigenvalues of the system. These equations are separated as

$$\frac{d\theta_{1n}}{dt} + \lambda_n^2 \theta_{1n} = 0 \text{ and } \frac{d\theta_{2n}}{dt} + \lambda_n^2 \theta_{2n} = 0 \tag{8}$$

and

$$\frac{1}{r} \left[\frac{dR_{1n}}{dr} + r \frac{d^2 R_{1n}}{dr^2} \right] + \frac{\lambda_n^2}{\alpha_{T1}} R_{1n} = 0$$

$$\frac{1}{r} \left[\frac{dR_{2n}}{dr} + r \frac{d^2 R_{2n}}{dr^2} \right] + \frac{\lambda_n^2}{\alpha_{T2}} R_{2n} = 0 \tag{9}$$

followed by the solutions

$$\theta_{1n} = C_{1n} e^{-\lambda_n^2 t} \text{ and } \theta_{2n} = C_{2n} e^{-\lambda_n^2 t} \tag{10}$$

and

$$R_{1n}(r) = A_{1n} J_0 \left(\frac{\lambda_n r}{\sqrt{\alpha_{T1}}} \right) + A_{2n} Y_0 \left(\frac{\lambda_n r}{\sqrt{\alpha_{T1}}} \right) \tag{11}$$

$$R_{2n}(r) = B_{1n} J_0 \left(\frac{\lambda_n r}{\sqrt{\alpha_{T2}}} \right) + B_{2n} Y_0 \left(\frac{\lambda_n r}{\sqrt{\alpha_{T2}}} \right) \tag{12}$$

where $J_0(r)$ and $Y_0(r)$ represent zero order Bessel functions of the first and second kind, respectively. As $Y_0(r)$ is not finite at $r = 0$; $A_{2n} = 0$, and the solutions in the radial dimension take the forms

$$R_{1n}(r) = A_{1n} J_0 \left(\frac{\lambda_n r}{\sqrt{\alpha_{T1}}} \right) \tag{13}$$

$$R_{2n}(r) = B_{1n} J_0 \left(\frac{\lambda_n r}{\sqrt{\alpha_{T2}}} \right) + B_{2n} Y_0 \left(\frac{\lambda_n r}{\sqrt{\alpha_{T2}}} \right) \tag{14}$$

since $R_{1n}(r)$ is an eigenfuction for any nonzero A_{1n}, we select $A_{1n} = 1$ for convenience. The interface and boundary conditions become

$$\begin{aligned} &R_{1n}(a) = R_{2n}(a) \\ &k_1 \frac{dR_{1n}(a)}{dr} = k_2 \frac{dR_{2n}(a)}{dr} \\ &k_2 \frac{dR_{2n}(b)}{dr} + hR_{2n}(b) = 0 \end{aligned} \tag{15}$$

Application of these conditions leads to

$$J_0 \left(\frac{a\lambda_n}{\sqrt{\alpha_{T1}}} \right) - B_{1n} J_0 \left(\frac{a\lambda_n}{\sqrt{\alpha_{T2}}} \right) - B_{2n} Y_0 \left(\frac{a\lambda_n}{\sqrt{\alpha_{T2}}} \right) = 0 \tag{16}$$

$$\begin{aligned} &\frac{k_1}{k_2} \sqrt{\frac{\alpha_{T2}}{\alpha_{T1}}} J_1 \left(\frac{a\lambda_n}{\sqrt{\alpha_{T1}}} \right) - B_{1n} J_1 \left(\frac{a\lambda_n}{\sqrt{\alpha_{T2}}} \right) \\ &\qquad - B_{2n} Y_1 \left(\frac{a\lambda_n}{\sqrt{\alpha_{T2}}} \right) = 0 \end{aligned} \tag{17}$$

$$\begin{aligned} &B_{1n} \left[hJ_0 \left(\frac{b\lambda_n}{\sqrt{\alpha_{T2}}} \right) - \frac{k_2 \lambda_n}{\sqrt{\alpha_{T2}}} J_1 \left(\frac{b\lambda_n}{\sqrt{\alpha_{T2}}} \right) \right] \\ &+ B_{2n} \left[hY_0 \left(\frac{b\lambda_n}{\sqrt{\alpha_{T2}}} \right) - \frac{k_2 \lambda_n}{\sqrt{\alpha_{T2}}} Y_1 \left(\frac{b\lambda_n}{\sqrt{\alpha_{T2}}} \right) \right] = 0 \end{aligned} \tag{18}$$

Letting

$$\beta = \frac{a}{\sqrt{\alpha_{T1}}},\quad \gamma = \frac{a}{\sqrt{\alpha_{T2}}},\quad K = \frac{k_1}{k_2}\sqrt{\frac{\alpha_{T2}}{\alpha_{T1}}},$$
$$\eta = \frac{b}{\sqrt{\alpha_{T2}}} \text{ and } H = \frac{h\sqrt{\alpha_{T2}}}{k_2} \tag{19}$$

these equations become

$$J_0(\beta\lambda_n) - B_{1n}J_0(\gamma\lambda_n) - B_{2n}Y_0(\gamma\lambda_n) = 0 \tag{20}$$
$$KJ_1(\beta\lambda_n) - B_{1n}J_1(\gamma\lambda_n) - B_{2n}Y_1(\gamma\lambda_n) = 0 \tag{21}$$

From the first two of these equations

$$\begin{bmatrix} J_0(\gamma\lambda_n) & Y_0(\gamma\lambda_n) \\ J_1(\gamma\lambda_n) & Y_1(\gamma\lambda_n) \end{bmatrix}\begin{bmatrix} B_{1n} \\ B_{2n} \end{bmatrix} = \begin{bmatrix} J_0(\beta\lambda_n) \\ KJ_1(\beta\lambda_n) \end{bmatrix} \tag{25}$$

B_{1n} and B_{1n} are determined as

$$B_{1n} = \frac{1}{\Delta}\left[J_0(\beta\lambda_n)Y_1(\gamma\lambda_n) - KJ_1(\beta\lambda_n)Y_0(\gamma\lambda_n)\right] \tag{26}$$
$$B_{2n} = \frac{1}{\Delta}\left[KJ_0(\gamma\lambda_n)J_1(\beta\lambda_n) - J_0(\beta\lambda_n)J_1(\gamma\lambda_n)\right] \tag{27}$$

where

$$\Delta = J_0(\gamma\lambda_n)Y_1(\gamma\lambda_n) - J_1(\gamma\lambda_n)Y_0(\gamma\lambda_n) \tag{28}$$

Eigenvalues are calculated from

$$\det[\mathbf{A}] = 0 \tag{29}$$

where **A** is the coefficient matrix given by Eq. (24). The result is

$$\begin{aligned} &Y_1(\gamma\lambda_n)\left[HJ_0(\beta\lambda_n)J_0(\eta\lambda_n) - \lambda_n J_0(\beta\lambda_n)J_1(\eta\lambda_n)\right] \\ &+ J_1(\gamma\lambda_n)\left[\lambda_n J_0(\beta\lambda_n)Y_1(\eta\lambda_n) - HJ_0(\beta\lambda_n)Y_0(\eta\lambda_n)\right] \\ &+ J_1(\beta\lambda_n)\{Y_0(\gamma\lambda_n)\left[K\lambda_n J_1(\eta\lambda_n) - HKJ_0(\eta\lambda_n)\right] \\ &+ J_0(\gamma\lambda_n)\left[HKY_0(\eta\lambda_n) - K\lambda_n Y_1(\eta\lambda_n)\right]\} = 0 \end{aligned} \tag{30}$$

The general solutions are then

$$T_1(r,t) = \sum_{n=1}^{\infty} C_n e^{-\lambda_n^2 t} R_{1n}(r) \tag{31}$$

$$T_2(r,t) = \sum_{n=1}^{\infty} C_n e^{-\lambda_n^2 t} R_{2n}(r) \tag{32}$$

$$\begin{aligned} &B_{1n}\left[HJ_0(\eta\lambda_n) - \lambda_n J_1(\eta\lambda_n)\right] \\ &+ B_{2n}\left[HY_0(\eta\lambda_n) - \lambda_n Y_1(\eta\lambda_n)\right] = 0 \end{aligned} \tag{22}$$

or in matrix notation

$$\mathbf{A}\times\begin{bmatrix} 1 \\ B_{1n} \\ B_{2n} \end{bmatrix} = \begin{bmatrix} 0 \\ 0 \\ 0 \end{bmatrix} \tag{23}$$

where the coefficient matrix is

$$\mathbf{A} = \begin{bmatrix} J_0(\beta\lambda_n) & -J_0(\gamma\lambda_n) & -Y_0(\gamma\lambda_n) \\ KJ_1(\beta\lambda_n) & -J_1(\gamma\lambda_n) & -Y_1(\gamma\lambda_n) \\ 0 & HJ_0(\eta\lambda_n) - \lambda_n J_1(\eta\lambda_n) & HY_0(\eta\lambda_n) - \lambda_n Y_1(\eta\lambda_n) \end{bmatrix} \tag{24}$$

It should be noted that since the time dependent functions θ_{1n} and θ_{2n} are independent of material properties of the layers, there is no discontinuity at the interface. Due to this reason in the above two equations instead of C_{1n} and C_{2n}, a single constant C_n is used. Application of the initial conditions leads to the equations

$$T_0 = \sum_{n=1}^{\infty} C_n R_{1n}(r) \tag{33}$$

$$T_0 = \sum_{n=1}^{\infty} C_n R_{2n}(r) \tag{34}$$

The orthogonality property is (Hahn and Özışık, 2012)

$$\begin{aligned} &\frac{k_1}{\alpha_{T1}}\int_0^a rR_{1n}(r)R_{1m}(r)dr \\ &+ \frac{k_2}{\alpha_{T2}}\int_a^b rR_{2n}(r)R_{2m}(r)dr = \begin{cases} 0 & for\ n \neq m \\ N_n & for\ n = m \end{cases} \end{aligned} \tag{35}$$

where the norm N_n is

$$N_n = \frac{k_1}{\alpha_{T1}}\int_0^a rR_{1n}^2(r)dr + \frac{k_2}{\alpha_{T2}}\int_a^b rR_{2n}^2(r)dr \tag{36}$$

The expression given in Eq. (35) is derived by using the two equations given in Eq. (9). Both of these equations are written for two different eigenvalues first. Then, the first set of these equations are multiplied by $R_{2n}(r)$, and the second set by $R_{1n}(r)$. The results are subtracted and integrated over the volume. The volume integrals are changed to surface integrals and the resulting expressions are summed up taking into consideration of the boundary conditions.

By performing integrations in Eq. (36) the norm N_n takes the form

$$N_n = E_1 + E_2 B_{1n}^2 + E_3 B_{1n} B_{2n} + E_4 B_{2n}^2 \tag{37}$$

where

$$E_1 = \frac{a^2 k_1}{2\alpha_{T1}}\left[J_0^2(\beta\lambda_n) + J_1^2(\beta\lambda_n)\right] \tag{38}$$

$$E_2 = \frac{k_2}{2\alpha_{T2}}\left\{b^2\left[J_0^2(\eta\lambda_n) + J_1^2(\eta\lambda_n)\right] - a^2\left[J_0^2(\gamma\lambda_n) + J_1^2(\gamma\lambda_n)\right]\right\} \tag{39}$$

$$E_3 = \frac{k_2}{\alpha_{T2}}\left\{b^2\left[J_0(\eta\lambda_n)Y_0(\eta\lambda_n) + J_1(\eta\lambda_n)Y_1(\eta\lambda_n)\right] - a^2\left[J_0(\gamma\lambda_n)Y_0(\gamma\lambda_n) + J_1(\gamma\lambda_n)Y_1(\gamma\lambda_n)\right]\right\} \tag{40}$$

$$E_4 = \frac{k_2}{2\alpha_{T2}}\left\{b^2\left[Y_0^2(\eta\lambda_n) + Y_1^2(\eta\lambda_n)\right] - a^2\left[Y_0^2(\gamma\lambda_n) + Y_1^2(\gamma\lambda_n)\right]\right\} \tag{41}$$

Multiplying both sides of Eqs. (33) and (34) by the operator

$$\frac{k_i}{\alpha_{Ti}} r R_{im}(r) \tag{42}$$

and integrating

$$\frac{k_1}{\alpha_{T1}}\int_0^a r T_0 R_{1m}(r)dr = \sum_{n=1}^{\infty} C_n\left[\frac{k_1}{\alpha_{T1}}\int_0^a r R_{1n}(r)R_{1m}(r)dr\right] \tag{43}$$

$$\frac{k_2}{\alpha_{T2}}\int_a^b r T_0 R_{2m}(r)dr = \sum_{n=1}^{\infty} C_n\left[\frac{k_2}{\alpha_{T2}}\int_a^b r R_{2n}(r)R_{2m}(r)dr\right] \tag{44}$$

adding for $m = n$

$$\frac{k_1 T_0}{\alpha_{T1}}\int_0^a r R_{1n}(r)dr + \frac{k_2 T_0}{\alpha_{T2}}\int_a^b r R_{2n}(r)dr = C_n N_n \tag{45}$$

or by integrations

$$I_1 + I_2 = C_n N_n \tag{46}$$

where

$$I_1 = \frac{k_1 T_0 \beta}{\lambda_n} J_1(\beta\lambda_n) \tag{47}$$

$$I_2 = \frac{k_2 T_0}{\sqrt{\alpha_{T2}}\lambda_n}\left\{B_{1n}\left[bJ_1(\eta\lambda_n) - aJ_1(\gamma\lambda_n)\right] + B_{2n}\left[bY_1(\eta\lambda_n) - aY_1(\gamma\lambda_n)\right]\right\} \tag{48}$$

then the solution is completed as

$$C_n = \frac{1}{N_n}(I_1 + I_2) \tag{49}$$

Temperature Distribution for Prescribed Surface Temperature

In this case the two-layer cylinder is mounted between rigid casing and cools down as it touches to the walls of the cooler casing. Hence, the conduction equations, Eqs. (1) and (2), are solved with the following boundary conditions

$$\begin{aligned} &T_1(0,t) = \text{ finite} \\ &T_2(b,t) = T_C \end{aligned} \tag{50}$$

where T_C represents the temperature of the casing. This nonhomogeneous boundary condition is made homogeneous by the introduction of new dependent variables

$$\phi_1(r,t) = T_1(r,t) - T_C \tag{51}$$

$$\phi_2(r,t) = T_2(r,t) - T_C \tag{52}$$

then the system to be solved becomes

$$\frac{\partial\phi_1}{\partial t} = \frac{\alpha_{T1}}{r}\left[\frac{\partial\phi_1}{\partial r} + r\frac{\partial^2\phi_1}{\partial r^2}\right] \text{ in } 0 \le r < a,\ t > 0 \tag{53}$$

$$\frac{\partial\phi_2}{\partial t} = \frac{\alpha_{T2}}{r}\left[\frac{\partial\phi_2}{\partial r} + r\frac{\partial^2\phi_2}{\partial r^2}\right] \text{ in } a < r < b,\ t > 0 \tag{54}$$

with the following conditions: boundary

$$\begin{aligned} &\phi_1(0,t) = \text{ finite} \\ &\phi_2(b,t) = 0 \end{aligned} \tag{55}$$

interface

$$\begin{aligned} &\phi_1(a,t) = \phi_2(a,t) \\ &k_1\frac{\partial\phi_1(a,t)}{\partial r} = k_2\frac{\partial\phi_2(a,t)}{\partial r} \end{aligned} \tag{56}$$

and initial

$$\begin{aligned} &\phi_1(r,0) = T_0 - T_C \\ &\phi_2(r,0) = T_0 - T_C \end{aligned} \tag{57}$$

The solution is realized by separation of variables as in the first problem. The result is

$$\phi_1(r,t) = \sum_{n=1}^{\infty} C_n e^{-\lambda_n^2 t} R_{1n}(r) \tag{58}$$

$$\phi_2(r,t) = \sum_{n=1}^{\infty} C_n e^{-\lambda_n^2 t} R_{2n}(r) \tag{59}$$

where the eigenfunctions $R_{1n}(r)$ and $R_{2n}(r)$ are given by Eqs. (13) - (14), respectively and

$$C_n = \frac{1}{N_n}\left(I_1 + I_2\right) \tag{60}$$

the norm N_n is the same as above, Eq. (37), and

$$I_1 = \frac{k_1\left(T_0 - T_C\right)\beta}{\lambda_n} J_1(\beta\lambda_n) \tag{61}$$

$$I_2 = \frac{k_2\left(T_0 - T_C\right)}{\sqrt{\alpha_{T2}}\lambda_n}\{B_{1n}\left[bJ_1(\eta\lambda_n) - aJ_1(\gamma\lambda_n)\right] + B_{2n}\left[bY_1(\eta\lambda_n) - aY_1(\gamma\lambda_n)\right]\} \tag{62}$$

The eigenvalues λ_n, for $n = 1,2,...$ of this solution are the roots of the nonlinear equation

$$\begin{aligned} &Y_0(\eta\lambda_n)\left[KJ_0(\gamma\lambda_n)J_1(\beta\lambda_n) - J_0(\beta\lambda_n)J_1(\gamma\lambda_n)\right] \\ &- J_0(\eta\lambda_n)\left[KJ_1(\beta\lambda_n)Y_0(\gamma\lambda_n) - J_0(\beta\lambda_n)Y_1(\gamma\lambda_n)\right] = 0 \end{aligned} \tag{63}$$

Finally, the temperature distributions are determined from

$$\begin{aligned} T_1(r,t) &= \phi_1(r,t) + T_C \\ T_2(r,t) &= \phi_2(r,t) + T_C \end{aligned} \tag{64}$$

Elastic Solutions

Basic equations

As the cylinder cools down slowly, the uncoupled theory of elasticity can be used. Hence, the equations of the generalized Hooke's law

$$\varepsilon_r = \frac{1}{E}\left[\sigma_r - \nu\left(\sigma_\theta + \sigma_z\right)\right] + \alpha\left(T - T_0\right) \tag{65}$$

$$\varepsilon_\theta = \frac{1}{E}\left[\sigma_\theta - \nu\left(\sigma_r + \sigma_z\right)\right] + \alpha\left(T - T_0\right) \tag{66}$$

$$\varepsilon_z = \frac{1}{E}\left[\sigma_z - \nu\left(\sigma_r + \sigma_\theta\right)\right] + \alpha\left(T - T_0\right) \tag{67}$$

the strain displacement relations

$$\varepsilon_\theta = \frac{u}{r} \;\; ; \;\; \varepsilon_r = \frac{du}{dr} \tag{68}$$

and the equation of equilibrium

$$\frac{d\sigma_r}{dr} + \frac{\sigma_r - \sigma_\theta}{r} = 0 \tag{69}$$

form the basic elastic equations for both regions (Timoshenko and Goodier, 1970; Rees, 1990). In these equations ε_j represents a strain component, E the modulus of elasticity, σ_j a normal stress component, ν the Poisson's ratio, α the coefficient of thermal expansion and T_0 the initial temperature as before. In case of generalized plane strain $\varepsilon_z = \varepsilon_0 = \text{constant}$, the axial stress turns into

$$\sigma_z = E\varepsilon_0 + \nu\left(\sigma_r + \sigma_\theta\right) - E\alpha\left(T - T_0\right) \tag{70}$$

Solutions in the following sections are carried out by the use of normalized and dimensionless variables. These are $\bar{r} = r/b$ dimensionless radial coordinate, $\tau = \alpha_{T1}t/b$ dimensionless time, $\bar{T}_j = T_j/T_0$ dimensionless temperature, $\bar{\varepsilon}_j = \varepsilon_j E_1/\sigma_{01}$ normalized strain component, $\bar{\sigma}_j = \sigma_j/\sigma_{01}$ dimensionless stress component, $\bar{u} = E_1 u/(\sigma_{01}b)$ dimensionless radial displacement, ν_j Poisson's ratio, $\bar{\alpha}_j = E_1\alpha_j T_0/\sigma_{01}$ dimensionless coefficient of thermal expansion, $\bar{E} = E_1/E_2$ ratio of moduli of elasticity and σ_{01} the uniaxial yield limit of the inner region material.

Solution for the inner region

Combining the equations of the generalized Hooke's law with the strain displacement relations and substituting the axial stress $\bar{\sigma}_z$ into these equations, the radial and circumferential stresses can be expressed in terms of displacement and its first order derivative as

$$\bar{\sigma}_r = \frac{1}{\left(1+\nu_1\right)\left(1-2\nu_1\right)}\left[\frac{\nu_1\bar{u}}{\bar{r}} + \left(1-\nu_1\right)\frac{d\bar{u}}{d\bar{r}} + \bar{\varepsilon}_0\nu_1\right] - \frac{\bar{\alpha}_1\left(\bar{T}_1 - 1\right)}{1-2\nu_1} \tag{71}$$

$$\bar{\sigma}_\theta = \frac{1}{\left(1+\nu_1\right)\left(1-2\nu_1\right)}\left[\frac{\left(1-\nu_1\right)\bar{u}}{\bar{r}} + \nu_1\frac{d\bar{u}}{d\bar{r}} + \bar{\varepsilon}_0\nu_1\right] - \frac{\bar{\alpha}_1\left(\bar{T}_1 - 1\right)}{1-2\nu_1} \tag{72}$$

Substituting these stresses in the equation of equilibrium the governing differential equation for the inner region is obtained as

$$\bar{r}^2\frac{d^2\bar{u}}{d\bar{r}^2} + \bar{r}\frac{d\bar{u}}{d\bar{r}} - \bar{u} = \frac{1+\nu_1}{1-\nu_1}\bar{\alpha}_1\bar{r}^2\frac{d\bar{T}_1}{d\bar{r}} \tag{73}$$

The general solution is

$$\bar{u}(\bar{r},\tau) = C_1\bar{r} + \frac{C_2}{\bar{r}} + \frac{\bar{\alpha}_1(1+\nu_1)}{1-\nu_1}\frac{F(\bar{r},\tau)}{\bar{r}} \tag{74}$$

where C_1 and C_2 are the arbitrary integration constants and

$$F(\bar{r},\tau)=\int_0^{\bar{r}}\xi\bar{T}_1(\xi,\tau)d\xi=\bar{r}\sqrt{\alpha_{T1}}\sum_{n=1}^{\infty}\frac{C_n}{\lambda_n}e^{-\lambda_n^2\tau}\left[J_1\left(\frac{\lambda_n\bar{r}}{\sqrt{\alpha_{T1}}}\right)\right] \tag{75}$$

Note that when $T_1=\phi_1+T_C$, the term $F(\bar{r},\tau)$ also includes the term $\bar{r}^2T_C/2$. We prefer using $F(\bar{r},\tau)$ instead of explicit result in Eq. (75) for the compactness of the latter lengthy equations. Meanwhile, it is to be noted that

$$\lim_{\bar{r}\to 0}\frac{F(\bar{r},\tau)}{\bar{r}}=\lim_{\bar{r}\to 0}\left[\bar{r}\bar{T}_1(\bar{r},\tau)\right]=\lim_{\bar{r}\to 0}\left\{\bar{r}\left[\phi_1(\bar{r},\tau)+T_C\right]\right\}=0 \tag{76}$$

Since the stresses and displacement must be finite at the center ($\bar{r}=0$), C_2 must be zero. Then the equations for the displacement and the stress components take the forms

$$\bar{u}(\bar{r},\tau)=C_1\bar{r}+\frac{\bar{\alpha}_1(1+\nu_1)}{1-\nu_1}\frac{F(\bar{r},\tau)}{\bar{r}} \tag{77}$$

$$\bar{\sigma}_r(\bar{r},\tau)=\frac{C_1+\bar{\varepsilon}_0\nu_1}{(1+\nu_1)(1-2\nu_1)}-\frac{\bar{\alpha}_1}{\bar{r}}\left[\frac{F(\bar{r},\tau)}{\bar{r}(1-\nu_1)}-\frac{F'(\bar{r},\tau)}{1-2\nu_1}\right]-\frac{\bar{\alpha}_1\left[\bar{T}_1(\bar{r},\tau)-1\right]}{1-2\nu_1} \tag{78}$$

$$\bar{\sigma}_\theta(\bar{r},\tau)=\frac{C_1+\bar{\varepsilon}_0\nu_1}{(1+\nu_1)(1-2\nu_1)}+\frac{\bar{\alpha}_1}{\bar{r}(1-\nu_1)}\left[\frac{F(\bar{r},\tau)}{\bar{r}}+\frac{\nu_1F'(\bar{r},\tau)}{1-2\nu_1}\right]-\frac{\bar{\alpha}_1\left[\bar{T}_1(\bar{r},\tau)-1\right]}{1-2\nu_1} \tag{79}$$

$$\bar{\sigma}_z(\bar{r},\tau)=\frac{2C_1\nu_1+\bar{\varepsilon}_0(1-\nu_1)}{(1+\nu_1)(1-2\nu_1)}+\frac{\bar{\alpha}_1\nu_1F'(\bar{r},\tau)}{\bar{r}(1-\nu_1)(1-2\nu_1)}-\frac{\bar{\alpha}_1\left[\bar{T}_1(\bar{r},\tau)-1\right]}{1-2\nu_1} \tag{80}$$

in these equations

$$F'(\bar{r},\tau)=\bar{r}\bar{T}_1(\bar{r},\tau) \tag{81}$$

or

$$F'(\bar{r},\tau)=\bar{r}\left[\phi_1(\bar{r},\tau)+T_C\right] \tag{82}$$

Solution for the outer region

Following similar steps as in the inner region, the solution is obtained as

$$\bar{\sigma}_r(\bar{r},\tau)=\frac{C_3+\bar{\varepsilon}_0\nu_2}{\bar{E}(1+\nu_2)(1-2\nu_2)}-\frac{C_4}{\bar{E}\bar{r}^2(1+\nu_2)}-\frac{\bar{\alpha}_2}{\bar{E}\bar{r}}\left[\frac{G(\bar{r},\tau)}{\bar{r}(1-\nu_2)}-\frac{G'(\bar{r},\tau)}{1-2\nu_2}\right]-\frac{\bar{\alpha}_2\left[\bar{T}_2(\bar{r},\tau)-1\right]}{\bar{E}(1-2\nu_2)} \tag{83}$$

$$\bar{\sigma}_\theta(\bar{r},\tau)=\frac{C_3+\bar{\varepsilon}_0\nu_2}{\bar{E}(1+\nu_2)(1-2\nu_2)}+\frac{C_4}{\bar{E}\bar{r}^2(1+\nu_2)}+\frac{\bar{\alpha}_2}{\bar{E}\bar{r}}\left[\frac{G(\bar{r},\tau)}{\bar{r}(1-\nu_2)}+\frac{\nu_2G'(\bar{r},\tau)}{(1-\nu_2)(1-2\nu_2)}\right]-\frac{\bar{\alpha}_2\left[\bar{T}_2(\bar{r},\tau)-1\right]}{\bar{E}(1-2\nu_2)} \tag{84}$$

$$\bar{\sigma}_z(\bar{r},\tau)=\frac{2C_3\nu_2+\bar{\varepsilon}_0(1-\nu_2)}{\bar{E}(1+\nu_2)(1-2\nu_2)}+\frac{\bar{\alpha}_2\nu_2G'(\bar{r},\tau)}{\bar{E}\bar{r}(1-\nu_2)(1-2\nu_2)}-\frac{\bar{\alpha}_2\left[\bar{T}_2(\bar{r},\tau)-1\right]}{\bar{E}(1-2\nu_2)} \tag{85}$$

where C_3 and C_4 are the arbitrary integration constants and

$$G(\bar{r},\tau)=\int_{\bar{a}}^{\bar{r}}\xi\bar{T}_2(\xi,\tau)d\xi=\sqrt{\alpha_{T2}}\sum_{n=1}^{\infty}\frac{C_n}{\lambda_n}e^{-\lambda_n^2\tau}\left\{B_{1n}\left[\bar{r}J_1\left(\frac{\lambda_n\bar{r}}{\sqrt{\alpha_{T2}}}\right)-\bar{a}J_1\left(\frac{\lambda_n\bar{a}}{\sqrt{\alpha_{T2}}}\right)\right]+B_{2n}\left[\bar{r}Y_1\left(\frac{\lambda_n\bar{r}}{\sqrt{\alpha_{T2}}}\right)-\bar{a}Y_1\left(\frac{\lambda_n\bar{a}}{\sqrt{\alpha_{T2}}}\right)\right]\right\} \tag{86}$$

Note that the term $\bar{r}^2T_C/2$ accompanies the right hand side of this equation if $T_2=\phi_2+T_C$. The derivatives of $G(\bar{r},\tau)$ are

$$G'(\bar{r},\tau)=\bar{r}\bar{T}_2(\bar{r},\tau) \tag{87}$$

or

$$G'(\bar{r},\tau)=\bar{r}\left[\phi_2(\bar{r},\tau)+T_C\right] \tag{88}$$

Evaluation of integration constants

Plane Strain In case of plane strain $\bar{\varepsilon}_0=0$ and the remaining constants C_1, C_3 and C_4 are evaluated from

$$\begin{aligned}&\bar{u}^I(\bar{a},\tau)=\bar{u}^{II}(\bar{a},\tau)\\&\bar{\sigma}_r^I(\bar{a},\tau)=\bar{\sigma}_r^{II}(\bar{a},\tau)\\&\bar{\sigma}_r^{II}(1,\tau)=0\end{aligned} \tag{89}$$

in which the superscripts *I* and *II* refer to inner and outer regions, respectively. Analytical expressions for the unknowns are determined by the comprehensive use of Mathematica. Since these expressions are overlong, it was not possible to include them here.

Generalized Plane Strain In this case $\bar{\varepsilon}_0 =$ constant, and the unknowns are C_1, C_3, C_4 and $\bar{\varepsilon}_0$. The three equations in the group by Eq. (89) are still valid and the additional equation is

$$\int_0^{\bar{a}} \bar{\sigma}_z^I(\bar{r},\tau)\bar{r}d\bar{r} + \int_{\bar{a}}^1 \bar{\sigma}_z^{II}(\bar{r},\tau)\bar{r}d\bar{r} = 0 \qquad (90)$$

Again, lengthy analytical expressions for the unknowns are determined by Mathematica.

Radially Constrained If the surface of the cylinder is mounted between rigid walls then the problem is a plane strain problem as well, i.e. $\bar{\varepsilon}_z = 0$ and the conditions are

$$\bar{u}^I(\bar{a},\tau) = \bar{u}^{II}(\bar{a},\tau)$$

$$\bar{\sigma}_r^I(\bar{a},\tau) = \bar{\sigma}_r^{II}(\bar{a},\tau)$$

$$\bar{u}^{II}(1,\tau) = 0 \qquad (91)$$

The three unknowns C_1, C_3 and C_4 are then evaluated analytically by the use of these equations. It should be noted that for the radially constrained case the cylinder is also assumed to be axially constrained so that the plane strain condition relative to r-θ plane exists.

PRESENTATION OF RESULTS

In the calculations, physical properties of two different engineering materials namely Aluminum (AL) and Brass (BR) are used. Numerical values of the properties of these materials are listed in Table 1. Dimensionless variables used in the calculations and in the presentation of the results are calculated by the use of the data given in Table 1.

Table 1. Physical properties of the materials used.

Physical Property	Symbol	Unit	Aluminum (AL)	Brass (BR)
Thermal diffusivity	α_T	m^2/s	9.5×10^{-5}	3.4×10^{-5}
Thermal conductivity	k	W/(m.°K)	230	110
Modulus of elasticity	E	GPa	70	105
Poisson's ratio	ν	-	0.35	0.35
Coeff. of thermal expansion	α	1/ °C	23.0×10^{-6}	20.9×10^{-6}
Uniaxial yield stress	σ_0	MPa	100	410

Plane Strain Calculations

In these calculations $T_0 = 60^0 C$, $h = 100$ W/(m^2 ^{0}K) and $\bar{a} = 0.6$ are used. Cooling of AL-BR and BR-AL cylinders from early times to steady state is plotted in Figs. 2(a) and 2(b), respectively. As seen in these figures the interface and boundary conditions are perfectly satisfied. While AL-BR cylinder reaches steady state at $\tau = 20.7$, BR-AL does at $\tau = 5.9$. There are two reasons for this difference. First one is that since the dimensionless time is determined from $\tau = \alpha_{T1} t/b$, the magnitude of α_{T1} affects calculation of τ, secondly the thermal conductivity of aluminum is twice as much as that of brass. Hence, if aluminum is in the outer layer cooling takes place more rapidly.

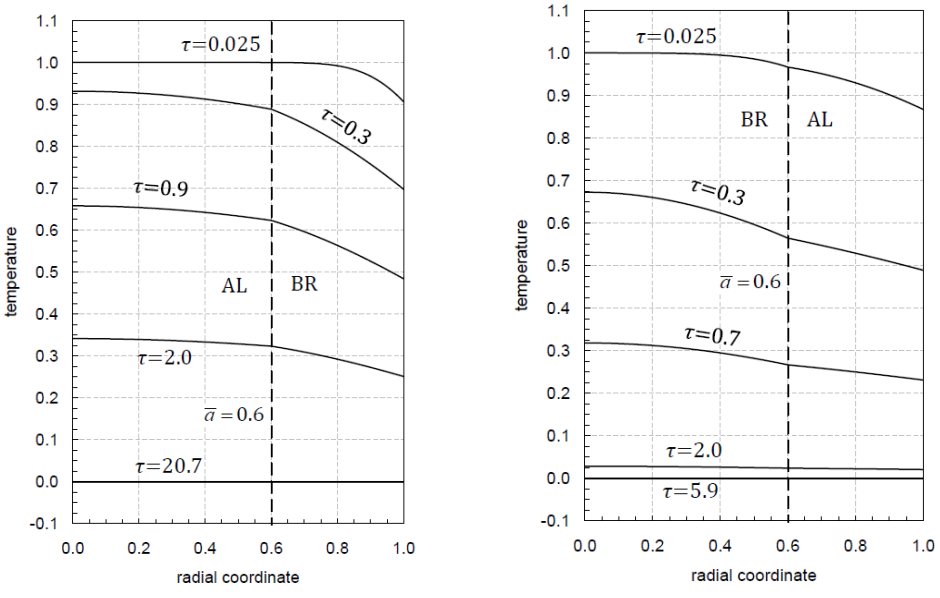

(a) (b)

Figure 2. Distributions of temperature for the (a) AL-BR (Aluminum-Brass), and (b) BR-AL (Brass-Aluminum) two-layer cylinders at various time instants for $\bar{a} = 0.6$ and $T_0 = 60^0 C$.

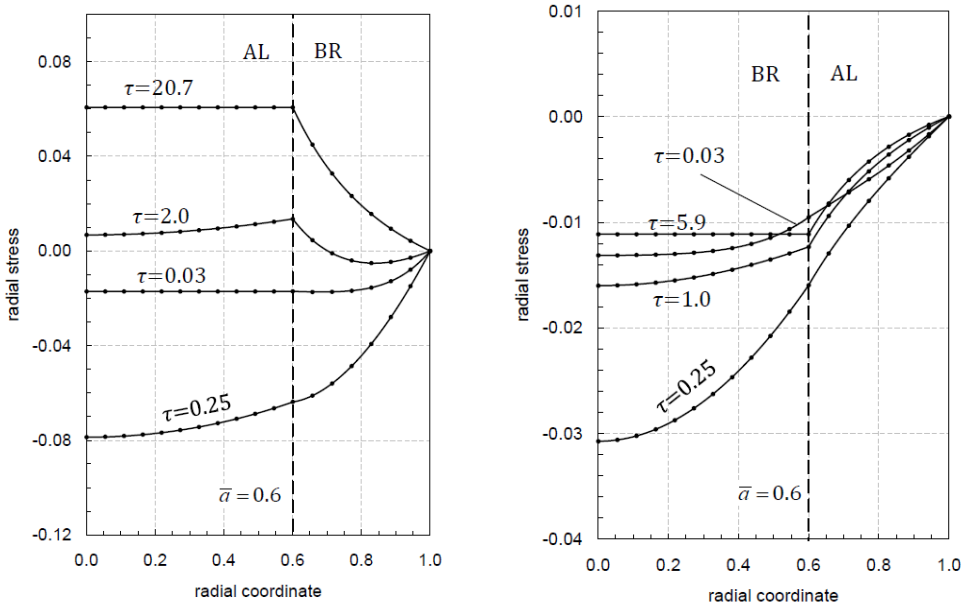

(a) (b)

Figure 3. Comparison of the variation of radial stress distributions for the (a) AL-BR (Aluminum-Brass), and (b) BR-AL (Brass-Aluminum) two-layer cylinders for plane strain and generalized plane strain cases at various time instants for $\bar{a} = 0.6$ and $T_0 = 60^0 C$. The solid lines belong to plane strain case and dots to generalized plane strain.

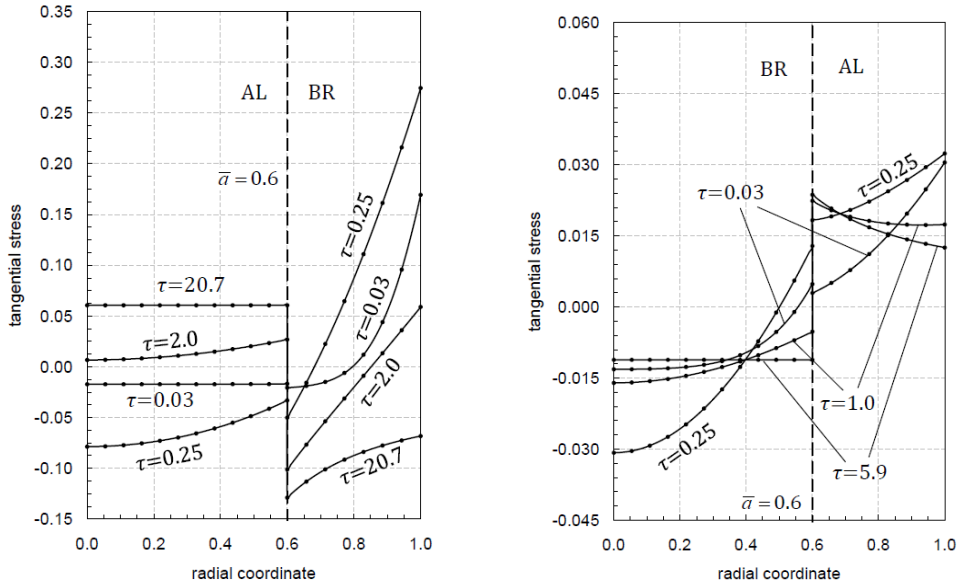

(a) (b)

Figure 4. Comparison of the variation of tangential stress distributions for the (a) AL-BR (Aluminum-Brass), and (b) BR-AL (Brass-Aluminum) two-layer cylinders for plane strain and generalized plane strain cases at various time instants for $\bar{a} = 0.6$ and $T_0 = 60^0 C$. The solid lines belong to plane strain case and dots to generalized plane strain.

The distributions of stress and displacement corresponding to temperature profiles in Figs. 2(a) and 2(b) are presented in Figs. 3 - 6. The details of these calculations are provided in Tables 2-5.

Table 2. Unknowns calculated for AL-BR (Aluminum-Brass) generalized plane strain two-layer cylinder for $\bar{a} = 0.6$.

τ	C_1	C_3	C_4	$\bar{\epsilon}_0$
0.025	-0.100365×10^1	-0.910570	0.327618	-0.152034×10^{-1}
0.03	-0.100375×10^1	-0.910380	0.327500	-0.181297×10^{-1}
0.25	-0.100293×10^1	-0.904712	0.301985	-0.131116
2.0	-0.977868	-0.887678	0.874624×10^{-1}	-0.630918
20.7	-0.963887	-0.878593	-0.307041×10^{-1}	-0.901851

Table 3. Unknowns calculated for BR-AL (Brass-Aluminum) generalized plane strain two-layer cylinder for $\bar{a} = 0.6$.

τ	C_1	C_3	C_4	$\bar{\varepsilon}_0$
0.025	-0.332142	-0.366973	0.131371	-0.166232×10^{-1}
0.03	-0.331933	-0.366926	0.130863	-0.197670×10^{-1}
0.25	-0.327211	-0.363207	0.943917×10^{-1}	-0.128406
0.3	-0.326519	-0.362455	0.871070×10^{-1}	-0.147228
1.0	-0.321412	-0.356844	0.327206×10^{-1}	-0.287133
5.9	-0.319532	-0.354777	0.126901×10^{-1}	-0.338643

Table 4. Unknowns calculated for the AL-BR (Aluminum-Brass) plane strain two-layer cylinder for $\bar{a} = 0.6$.

τ	C_1	C_3	C_4
0.025	-0.582071×10^{-2}	-0.456173×10^{1}	0.327618
0.03	-0.693840×10^{-2}	-0.456190×10^{1}	0.327500
0.25	-0.916629×10^{-1}	-0.428145×10^{1}	0.301985
2.0	-0.856437	-0.228657×10^{1}	-0.874624×10^{-1}
20.7	-0.127953×10^{1}	-0.119426×10^{1}	-0.307041×10^{-1}

The comparison of radial stress distributions in plane strain and in generalized plane strain calculations as time increases are plotted in Figs. 3(a) and 3(b). In these figures dots belong to the results of generalized plane strain calculations and solid lines to plane strain calculations. With low magnitudes, the results of these calculations are identical. The same situation is observed for tangential stress as well. The results of plane strain (solid lines) and generalized plane strain (dots) are presented in Figs. 4(a) and 4(b). The difference between axial stress distributions is obvious and can be visualized in Figs. 5(a) and 5(b). In these figures solid lines belong to the results of plane strain calculations and dashed lines to generalized plane strain. It is observed that sharp gradients dominate generalized plane strain calculations. The distributions of radial displacement for both calculations are plotted in Figs. 6(a) and 6(b). In these figures solid lines show the distributions for the plane strain case in which $\varepsilon_z = 0$.

Table 5. Unknowns calculated for the BR-AL (Brass-Aluminum) plane strain two-layer cylinder for $\bar{a} = 0.6$.

τ	C_1	C_3	C_4
0.025	-0.448840×10^{-2}	-0.179154×10^{1}	0.131371
0.03	-0.545516×10^{-2}	-0.177732×10^{1}	0.130863
0.25	-0.126000	-0.131818×10^{1}	0.943917×10^{-1}
0.3	-0.153701	-0.124240×10^{1}	0.871070×10^{-1}
1.0	-0.361493	-0.680260	0.327206×10^{-1}
5.9	-0.438051	-0.473325	0.126901×10^{-1}

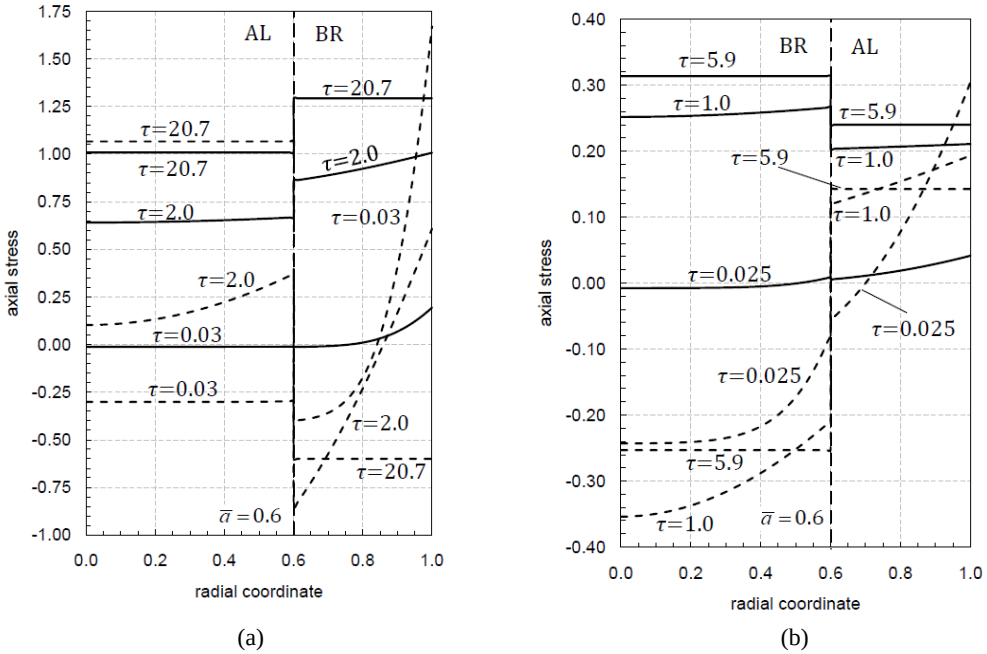

(a) (b)

Figure 5. Comparison of the variation of axial stress distributions for the (a) AL-BR (Aluminum-Brass), and (b) BR-AL (Brass-Aluminum) two-layer cylinders for plane strain and generalized plane strain cases at various time instants for $\bar{a} = 0.6$ and $T_0 = 60^0 C$. The solid lines belong to plane strain case and dashed lines to generalized plane strain. The stress values for the generalized plane strain case is multiplied by 10.

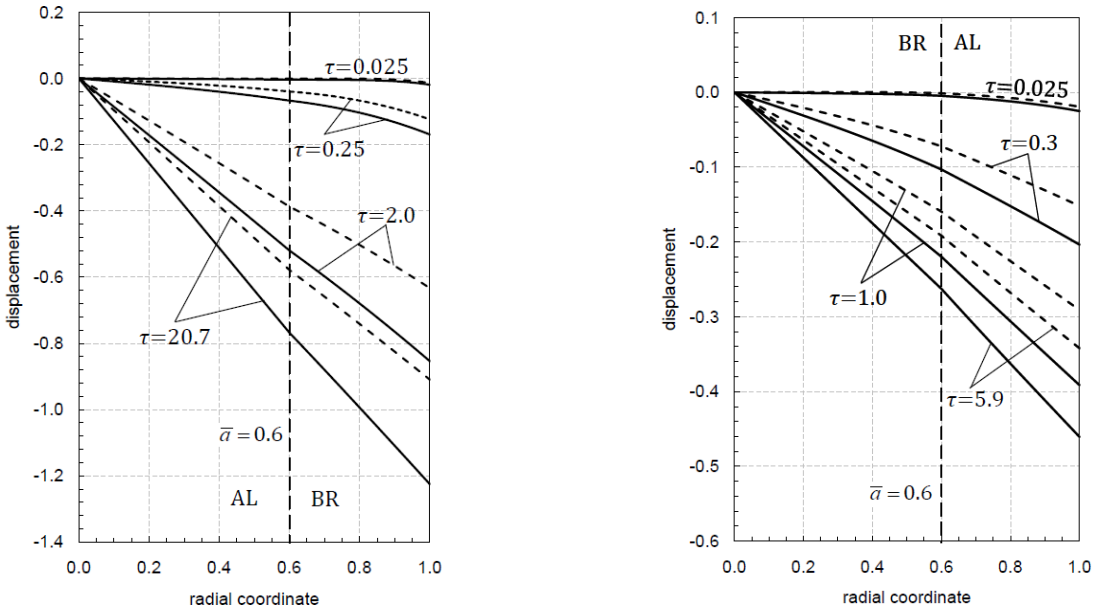

(a) (b)

Figure 6. Comparison of the distributions of radial displacement for the (a) AL-BR (Aluminum-Brass), and (b) BR-AL (Brass-Aluminum) two-layer cylinders for plane strain and generalized plane strain cases at various time instants for $\bar{a} = 0.6$ and $T_0 = 60^0 C$. The solid lines belong to plane strain case and dashed lines to generalized plane strain.

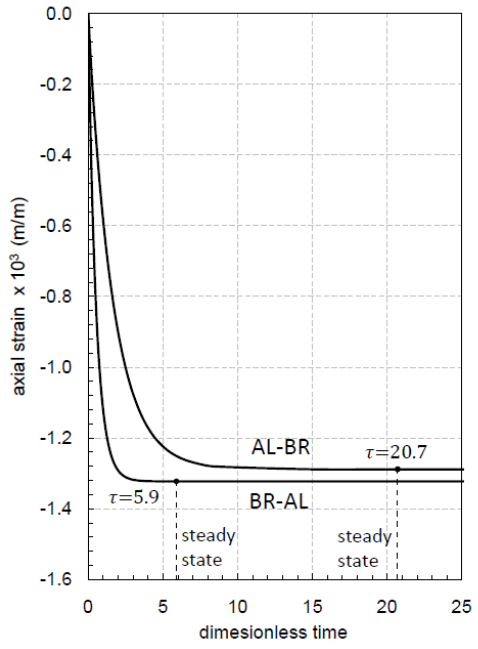

Figure 7. Variation of axial strain ($\varepsilon_0 = \bar{\varepsilon}_0 \sigma_{01} / E_1$) with time for AL-BR (Aluminum-Brass) and BR-AL (Brass-Aluminum) two-layer cylinders for generalized plane strain case ($\bar{a} = 0.6$ and $T_0 = 60^0 C$).

As seen in Figs. 6(a) and 6(b) when $\varepsilon_z = 0$ the contraction in volume is realized by contraction in the radial dimension only. However, in generalized plane strain case the cylinder contracts in both axial and radial dimensions. This situation is also illustrated in Fig. 7, on which the decrease in the axial dimension with time is plotted.

To check if the cylinder is deforming plastically with the calculated stresses, von Mises yield criterion is used. The von Mises stress, $\bar{\sigma}_{vM}$, is determined at any radial location using slightly different expressions for the inner and outer regions. For the inner region it is determined from

$$\bar{\sigma}_{vM} = \sqrt{\frac{1}{2}\left[(\bar{\sigma}_r - \bar{\sigma}_\theta)^2 + (\bar{\sigma}_r - \bar{\sigma}_z)^2 + (\bar{\sigma}_\theta - \bar{\sigma}_z)^2\right]} \quad (92)$$

while for the outer layer

$$\bar{\sigma}_{vM} = \left(\frac{\sigma_{01}}{\sigma_{02}}\right)\sqrt{\frac{1}{2}\left[(\bar{\sigma}_r - \bar{\sigma}_\theta)^2 + (\bar{\sigma}_r - \bar{\sigma}_z)^2 + (\bar{\sigma}_\theta - \bar{\sigma}_z)^2\right]} \quad (93)$$

where σ_{02} stands for the uniaxial yield stress of the material in this layer. Note that the cylinder becomes plastic at locations where $\bar{\sigma}_{vM} \geq 1$. The variations of $\bar{\sigma}_{vM}$ in the AL-BR and BR-AL cylinders at various time instants for both end conditions are calculated and plotted in Figs. 8(a), 8(b), 9(a) and 9(b). As seen in these figures, for both end conditions the stress states are elastic. In addition, larger magnitudes of von Mises stress are calculated in plane stress case for both cylinders.

Next, the results of the calculations for radially constrained plane strain two-layer cylinders are presented. Here the values $T_0 = 60^0 C$, $T_C = 12^0 C$ and

$\bar{a} = 0.5$ are used. Temperature distribution vs. time history of AL-BR cylinder is plotted in Fig. 10(a). As seen in this figure, $\bar{T}(\bar{r}) = T_C / T_0 = 0.2$ throughout in the cylinder when the steady state condition is reached at $\tau = 4.93$. To determine the corresponding stresses in the cylinder integration constants are determined and tabulated in Table 6.

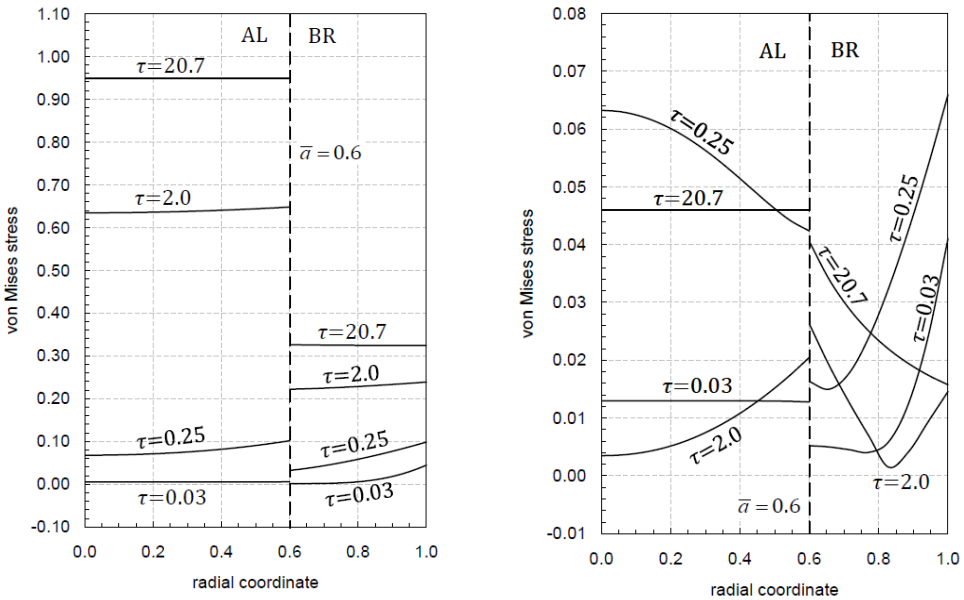

(a) (b)

Figure 8. Distributions of von Mises stress for the AL-BR (Aluminum-Brass) two-layer cylinders for (a) plane strain, and (b) generalized plane strain cases at various time instants for $\bar{a} = 0.6$ and $T_0 = 60^0 C$.

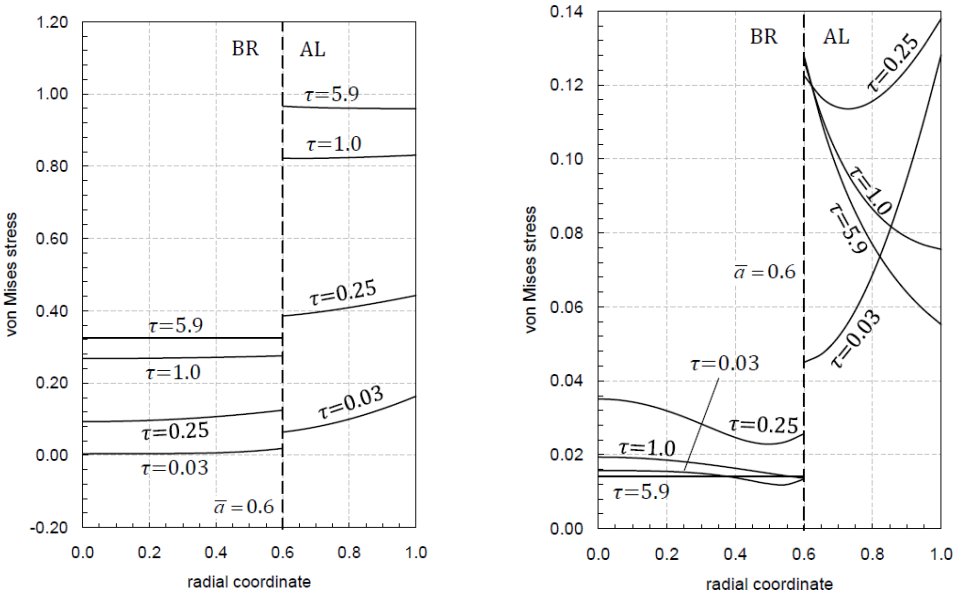

(a) (b)

Figure 9. Distributions of von Mises stress for the BR-AL (Brass-Aluminum) two-layer cylinders for (a) plane strain, and (b) generalized plane strain cases at various time instants for $\bar{a} = 0.6$, $T_0 = 60^0 C$.

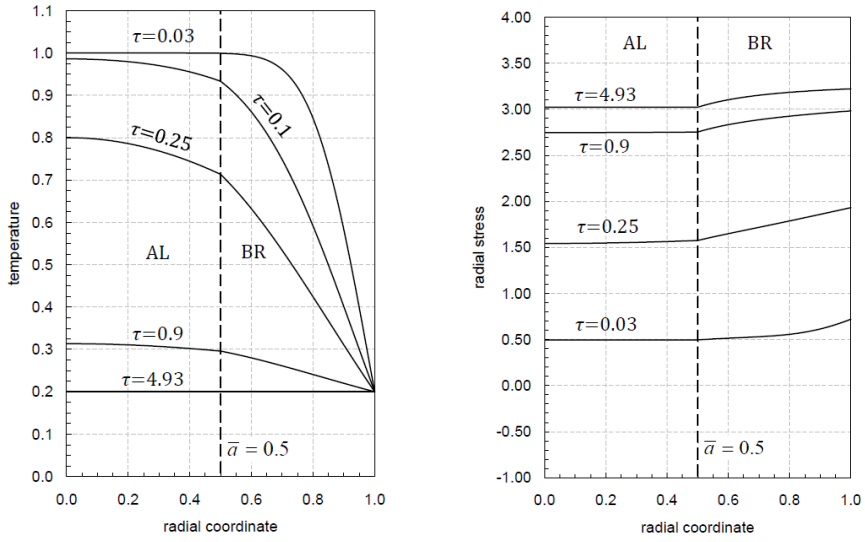

(a)

(b)

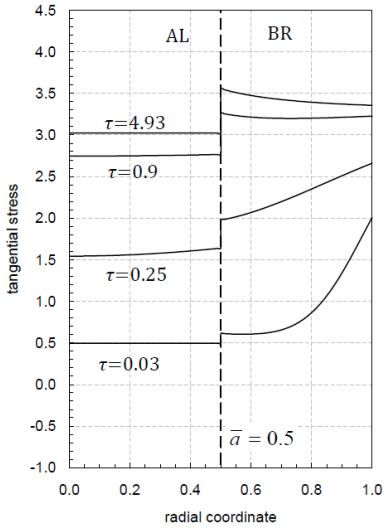

(c)

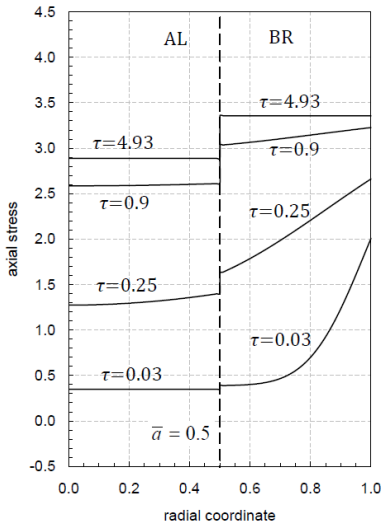

(d)

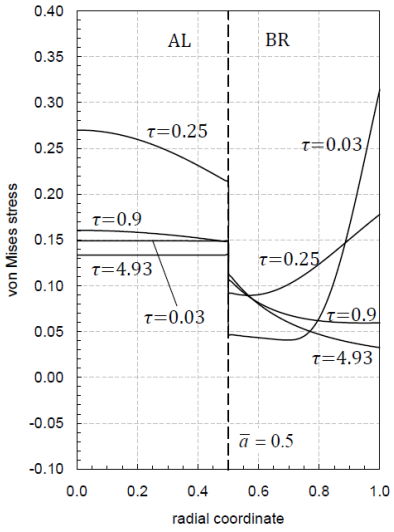

(e)

Figure 10. Distributions of (a) temperature, (b) radial stress, (c) tangential stress, (d) axial stress, and (e) von Mises stress for the AL-BR (Aluminum-Brass) axially and radially constrained two-layer cylinders (plane strain case) at various time instants for $\bar{a} = 0.5$, $T_0 = 60^0 C$, $T_C = 12^0 C$.

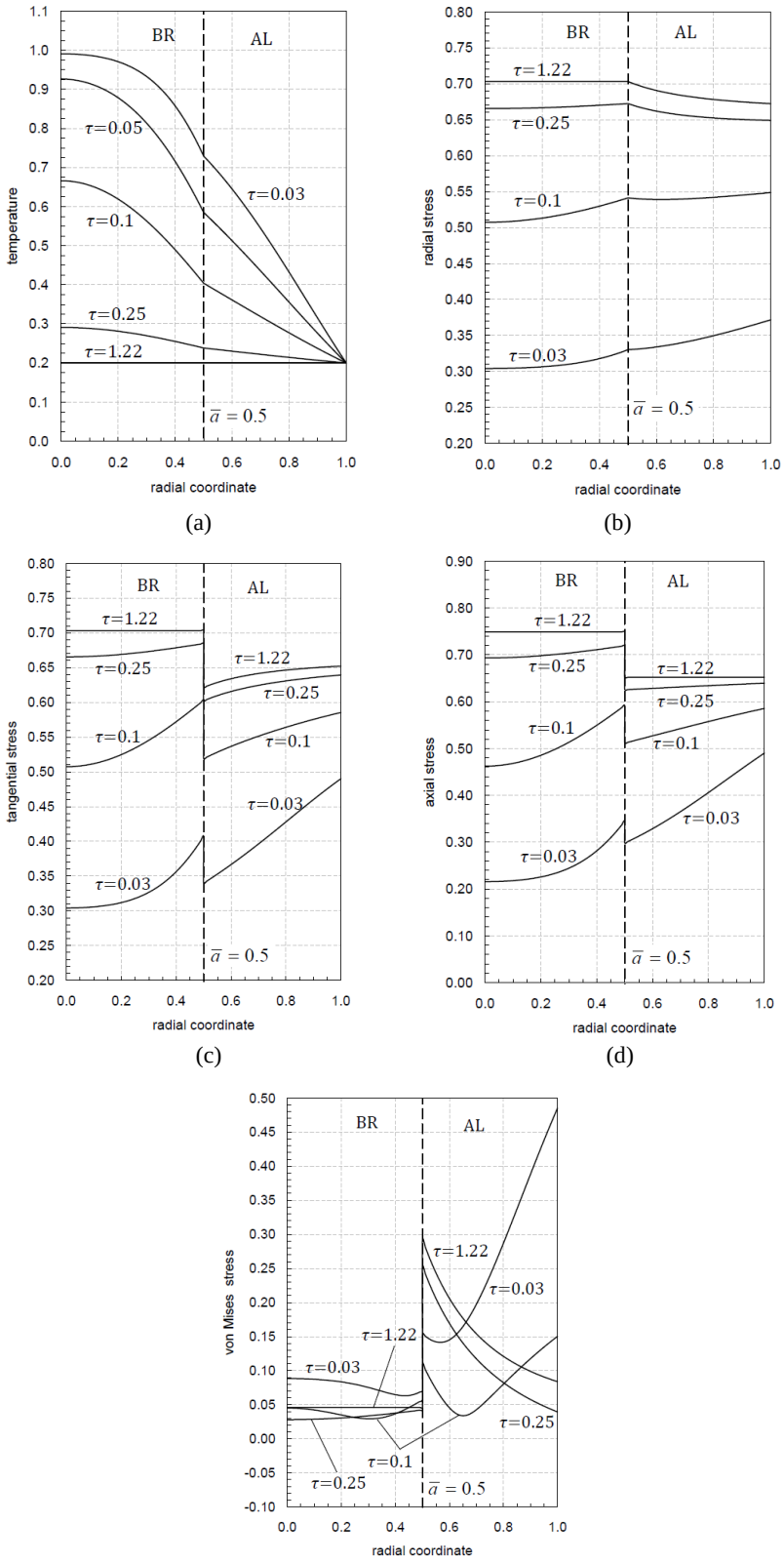

Figure 11. Distributions of (a) temperature, (b) radial stress, (c) tangential stress, (d) axial stress, and (e) von Mises stress for the BR-AL (Brass-Aluminum) axially and radially constrained two-layer cylinders (plane strain case) at various time instants for $\bar{a} = 0.5$, $T_0 = 60^0 C$, $T_C = 12^0 C$.

Table 6. Unknowns calculated for AL-BR (Aluminum-Brass) radially constrained plane strain cylinder for $\bar{a} = 0.5$.

τ	C_1	C_3	C_4
0.03	-0.801893	-0.761918	0.240756
0.1	-0.644804	-0.648036	0.242042
0.25	-0.438352	-0.510367	0.207737
0.9	-0.979417×10^{-1}	-0.292115	0.124936
4.93	-0.202731×10^{-1}	-0.242434	0.105699

Distributions of radial, tangential and axial stresses are plotted in Figs. 10(b), (c) and (d). The constraint in the radial direction gives rise to large magnitudes of the stresses. To check if the cylinder is deforming plastically with these large magnitudes of the stresses, the variations of $\bar{\sigma}_{vM}$ in the cylinder as time passes are calculated and plotted in Fig. 10(e). As seen in this figure, although the stresses have large magnitudes, the corresponding stress state is far away from plasticization.

Similar calculations are performed for Brass-Aluminum (BR-AL) radially constrained plane strain cylinder. The temperature profiles from early times to steady state are plotted in Fig. 11(a). BR-AL cylinder comes to steady state at τ = 1.22. Integration constants for this cylinder are calculated and tabulated in Table 7.

Table 7. Unknowns calculated for BR-AL (Brass-Aluminum) radially constrained plane strain cylinder for $\bar{a} = 0.5$.

τ	C_1	C_3	C_4
0.03	-0.211227	-0.193295	0.693263×10^{-1}
0.05	-0.189389	-0.158316	0.557702×10^{-1}
0.1	-0.161368	-0.110541	0.313801×10^{-1}
0.25	-0.134912	-0.636878×10^{-1}	0.413571×10^{-2}
1.22	-0.128746	-0.527198×10^{-1}	-0.233146×10^{-2}

Figs. 11(b) - 11(e) display the distributions of radial, tangential, axial and von Mises stresses, respectively. As seen in Fig. 11(e), again, the stress state is purely elastic.

CONCLUDING REMARKS

Using physical properties of Aluminum and Brass, plane strain, generalized plane strain, radially constrained plane strain thermoelastic analyses of the cooling of a two-layer cylinder are performed using the uncoupled theory of elasticity. The cylinder consists of two layers that are in perfect contact. In plane strain and generalized plane strain calculations it is supposed that the hot assembly loses energy from its surface to the zero ambient by convection. In these calculations, it is observed that while radial and circumferential stresses are very small in magnitude and are identical, the axial stress is the largest one among the principle stresses. Axial stress profiles in plane strain and in generalized plane strain differ to some extend with sharper gradients in the state of generalized plane strain. On the other hand, for both end conditions it is observed that the stress states from early times to steady state are elastic when the von Mises citerion is considered.

In the solutions with radially constrained boundary condition, the cylinder is assumed to be mounted between rigid walls. Cooling of the cylinder takes place as it touches cooler surface of the rigid casing. In this case the decrease in length is not possible and the problem becomes a plane strain one at the same time. Radially constrained boundaries give rise to stresses with large magnitudes but it is shown by the use of von Mises yield condition that the resulting stress state is far away form plasticization.

REFERENCES

Boley B. A. and Weiner, J. H., 1960, *Theory of Thermal Stresses*, Wiley, New York.

Carslaw H. S. and Jaeger J. C., 1959, *Conduction of Heat in Solids* (Sec. Ed.), Oxford University Press, Oxford.

Eraslan A. N. and Apatay T., 2015, Thermoelastic Stresses in a Rod Subjected to Periodic Boundary Condition: An Analytical Treatment, *J. Multidisciplinary Eng. Sci. Tech.*, 2, 2438-2444.

Eraslan A. N and Apatay T., 2016, Analytical Solution to Thermal Loading and Unloading of a Cylinder Subjected to Periodic Surface Heating, *J. Thermal Stresses*, 39, 928-941.

Eraslan A. N. and Apatay T., 2017, Thermal Loading and Unloading of a Solid Cylinder Subjected to Periodic Internal Energy Cycling, *ZAMM*, 97, 340-357.

Hahn W. D. and Özışık M. N., 2012, *Heat Conduction*, John Wiley & Sons, New Jersey.

Hetnarski B. H. and Eslami M. R., 2009, *Thermal Stresses-Advanced Theory and Applications*, Springer, Netherlands.

Ishikawa H., 1978, A Thermoelastoplastic Solution for a Circular Solid Cylinder Subjected to Heating and Cooling, *J. Thermal Stresses*, 1, 211-222.

Jane K. C. and Lee Z. Y., 1999, Thermoelastic Transient Response of an Infinitely Long Annular Multilayered Cylinder, *Mech. Res. Comm.*, 26, 709-718.

Kandil A., El-Kady A. A. and El-Kafrawy A., 1995, Transient Thermal Stress Analysis of Thick-Walled Cylinders, *Int. J. Mech. Sci.*, 37, 721-732.

Lee Z. Y., 2006, Generalized Coupled Transient Thermoelastic Problem of Multilayered Hollow Cylinder with Hybrid Boundary Conditions, *Int. Comm. Heat Mass Transfer*, 33, 518-528.

Lee Z. -Y., Chen C. K. and Hung C. -I., 2001, Transient Thermal Stress Analysis of Multilayered Hollow Cylinder, *Acta Mechanica*, 151, 75-88.

Lu X., Tervola P. and Viljanen M., 2006a, Transient Analytical Solution to Heat Conduction in Composite Circular Cylinder, *Int. J. Heat Mass Transfer*, 49, 341-348.

Lu X., Tervola P. and Viljanen M., 2006b, Transient Analytical Solution to Heat Conduction in Multi-Dimensional Composite Cylinder Slab, *Int. J. Heat Mass Transfer*, 49, 1107-1114.

Lu X. and Viljanen M., 2006, An Analytical Method to Solve Heat Conduction in Layered Spheres with Time-Dependent Boundary Conditions, *Phys. Lett. A*, 351, 274-282.

Mashat D. S., Zenkour A. M. and Elsibai K. A., 2010, Transient Response of Multilayered Hollow Cylinder Using Various Theories of Generalized Thermoelasticity, *Natural Science*, 2, 1171-1179.

Monte F. D., 2002, An Analytic Approach to the Unsteady Heat Conduction Processes in One-Dimensional Composite Media, *Int. J. Heat Mass Transfer*, 45, 1333-1343.

Noda N., Hetnarski R. B. and Tanigawa Y., 2003, *Thermal Stresses* (Sec. Ed.), Taylor and Francis, New York.

Özışık M. N., 1980, *Heat Conduction*, Wiley, New York.

Pardo E., Sarmiento G. S., Laura P. A. A. and Gutierrez R. H., 1987, Analytical Solution for Unsteady Thermal Stresses in an Infinite Cylinder Composed of Two Materials, *J. Thermal Stresses*, 10, 29-43.

Rees D. W. A., 1990, *The Mechanics of Solids and Structures*, McGraw-Hill, London, New York.

Singh S., Jain P. K. and Rizwan-uddin, 2008, Analytical Solution to Transient Heat Conduction in Polar Coordinates with Multiple Layers in Radial Direction, *Int. J. Therm. Sci.*, 47, 261-273.

Sun Y. and Wichman I. S., 2004, On Transient Heat Conduction in a One-Dimensional Composite Slab, *Int. J. Heat Mass Transfer*, 47, 1555-1559.

Tanigawa Y., Takeuti Y. and Ueshima K., 1984, Transient Thermal Stresses of Solid and Hollow Spheres with Spherically Isotropic Thermoelastic Properties, *Ingenieur-Archiv*, 54, 259-267.

Thomas J. R., Singh J. P., Tawil H., Powers L. and Hasselma D. P. H., 1985, Thermal Stresses in a Long Circular Cylinder Subjected to Sudden Cooling During Transient Convection Heating, *J. Thermal Stresses*, 8, 249-260.

Timoshenko S. and Goodier J. N., 1970, *Theory of Elasticity*, McGraw-Hill, New-York.

Wang H. M., Ding H. J. and Chen Y. M., 2004, Thermoelastic Dynamic Solution of a Multilayered Spherically Isotropic Hollow Sphere for Spherically Symmetric Problems, *Acta Mechanica*, 173, 131-145.

Yu-Ching Y. and Cha'o-Kuang C., 1986, Thermoelastic Transient Response of Infinitely Long Annular Cylinder Composed of Two Different Materials, *Int. J. Eng. Sci.*, 24, 569-581.